

\mathcal{CP} violation in semi-leptonic B decays at LHCb

Thomas Bird (*On behalf of the LHCb collaboration*)

The School of Physics and Astronomy, The University of Manchester, Oxford Road,
Manchester, M13 9PL, UK

E-mail: thomas.bird@cern.ch

Abstract. Three methods of measuring the \mathcal{CP} violating quantities a_{fs}^s and a_{fs}^d are discussed. The LHCb experiment is used to measure semi-leptonic B_d and B_s decays from pp collisions created by the Large Hadron Collider. The flavour specific decays of $B_s \rightarrow D_s(\phi\pi)\mu\nu$ are selected and the final state charge asymmetry is measured, which to first order is proportional to a_{fs}^s . This is done by fitting the $KK\pi$ invariant mass distributions to determine the yield of both $D_s^+\mu^-$ and $D_s^-\mu^+$ events. The charge-dependant efficiency for selecting this decay is measured using data-driven techniques. Using this information, the yields are corrected and the final state charge asymmetry is obtained, resulting in $a_{fs}^s = (-0.24 \pm 0.54 \pm 0.33)\%$. Finally two proposed LHCb measurements are described: a time-dependent difference and sum measurement $a_{fs}^s \pm a_{fs}^d$ and a time-dependent measurement of a_{fs}^d .

1. Introduction

There are two neutral B mesons, the B_s meson and the B_d meson. In the following these will generically be denoted as B_q . The B_q meson has two flavour eigenstates $|B^0\rangle$ and $|\overline{B}^0\rangle$, the time evolution of which is governed by the following equation:

$$i \frac{d}{dt} \begin{pmatrix} |B^0\rangle \\ |\overline{B}^0\rangle \end{pmatrix} = \left(\hat{M} - \frac{i}{2} \hat{\Gamma} \right) \begin{pmatrix} |B^0\rangle \\ |\overline{B}^0\rangle \end{pmatrix}.$$

In the absence of mixing one expects \hat{M} and $\hat{\Gamma}$ to be diagonal matrices; however off-diagonal elements M_{12} and Γ_{12} arise from the Feynman diagrams shown in figure 1. Diagonalisation of \hat{M} and $\hat{\Gamma}$ gives two mass eigenstates: a light one, $|B_L\rangle$, and a heavy one, $|B_H\rangle$. These are related to the flavour eigenstates by

$$|B_L\rangle = p|B^0\rangle + q|\overline{B}^0\rangle \quad \text{and} \quad |B_H\rangle = p|B^0\rangle - q|\overline{B}^0\rangle.$$

Three observables describe \mathcal{CP} violation and mixing in B_q mesons. First is the mass difference between the heavy and the light eigenstates, $\Delta m_q = M_H - M_L = 2|M_{12}|$, then the difference in decay widths of the two eigenstates, $\Delta\Gamma_q = \Gamma_L - \Gamma_H \approx 2|\Gamma_{12}| \cos \phi$, where ϕ is the phase between M_{12} and Γ_{12} , and finally the flavour specific asymmetry, $a_{fs}^q = |\Gamma_{12}|/|M_{12}| \sin \phi \approx -2(|q/p| - 1)$, which will be the focus of the following analyses. The Standard Model predicts [1] these two observables to be close to zero, specifically

$$a_{fs}^s = (1.9 \pm 0.3) \times 10^{-5} \quad \text{and} \quad a_{fs}^d = -(4.1 \pm 0.6) \times 10^{-4}.$$



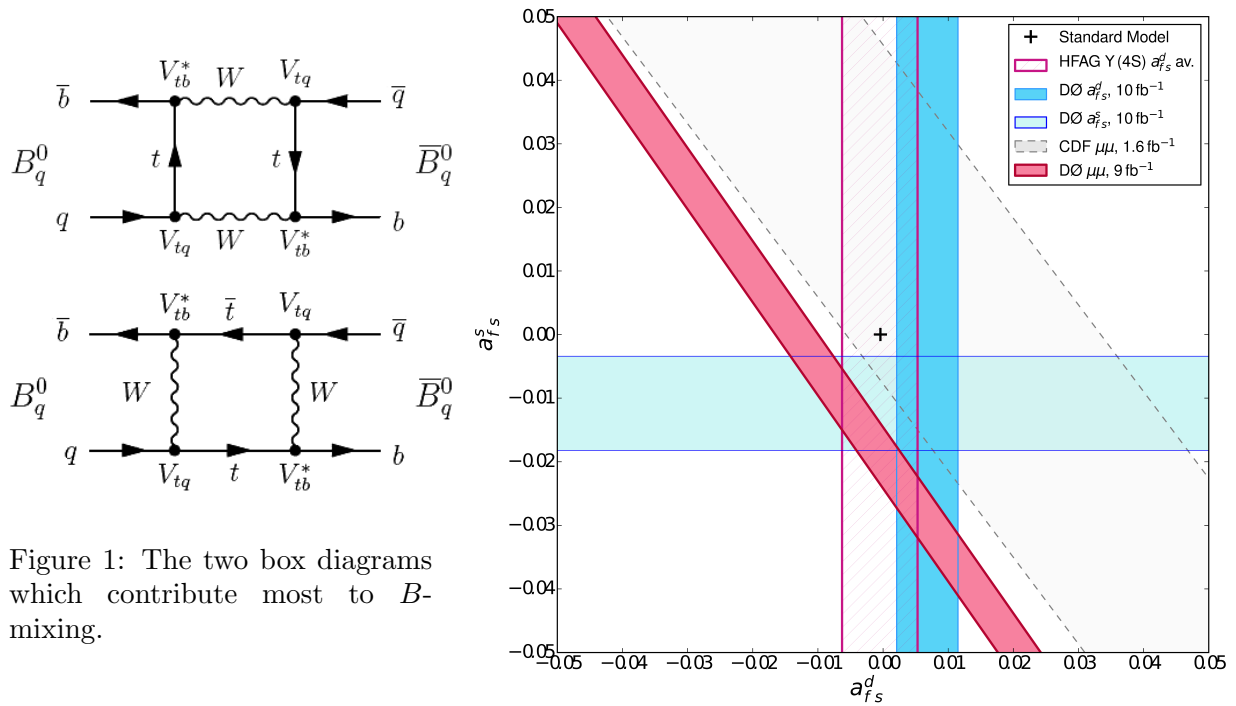


Figure 1: The two box diagrams which contribute most to B -mixing.

Figure 2: Plot in the $a_{fs}^s - a_{fs}^d$ plane showing CDF and DØ measurements along with an average of the B -factory measurements from HFAG and the Standard Model prediction. The horizontal (vertical) lines are direct measurements of a_{fs}^s (a_{fs}^d) and the diagonal lines show a measurement of the linear combination of a_{fs}^s and a_{fs}^d .

This asymmetry is also called a_{sl}^q when measured using semi-leptonic decays such as:

$$a_{fs}^q \rightarrow a_{sl}^q \propto \frac{N(\overline{B}_q^0(t) \rightarrow D_q^+ \mu^- \bar{\nu}) - N(B_q^0(t) \rightarrow D_q^- \mu^+ \nu)}{N(\overline{B}_q^0(t) \rightarrow D_q^+ \mu^- \bar{\nu}) + N(B_q^0(t) \rightarrow D_q^- \mu^+ \nu)}.$$

2. Previous measurements

There have been many different measurements of a_{fs}^s and a_{fs}^d . Figure 2 shows a selection of them. The horizontal (vertical) lines are measurements of a_{fs}^s (a_{fs}^d) and the diagonal lines are measurements of a linear combination of a_{fs}^s and a_{fs}^d . Of these measurements the most interesting is the DØ di-muon asymmetry [2], which is a linear combination of a_{fs}^s and a_{fs}^d . DØ measured $A_{sl}^b = (-0.787 \pm 0.172 \pm 0.093)\% = (0.594 \pm 0.022)a_{fs}^d + (0.406 \pm 0.022)a_{fs}^s$, which differs from the Standard Model prediction by 3.9 standard deviations.

3. LHCb detector

LHCb is a single-arm spectrometer [3] at the Large Hadron Collider (LHC), a proton-proton collider which in 2011 operated at a centre-of-mass energy of $\sqrt{s} = 7$ TeV. A schematic of the LHCb detector is shown in figure 3, where it can be seen that the acceptance covers high pseudorapidities, compared to the general purpose detectors, specifically $2 < \eta < 5$. The Vertex Locator (VELO) is able to achieve an average resolution of $\sim 10 \mu m$ ($\sim 60 \mu m$) on the primary vertex position [4] in the direction perpendicular (parallel) to the beam pipe. This is used

to measure the flight distance of a particle, which is proportional to the decay time. LHCb has a magnet, the polarity of which can be changed. This is used to help correct for charge asymmetries caused by different detection efficiencies for positive or negative particles. LHCb is also able to discriminate between pions and kaons using particle identification provided mainly by the Ring Imaging Cherenkov (RICH) detectors. Finally the muon stations are used to trigger events containing semi-leptonic decays and to identify muons.

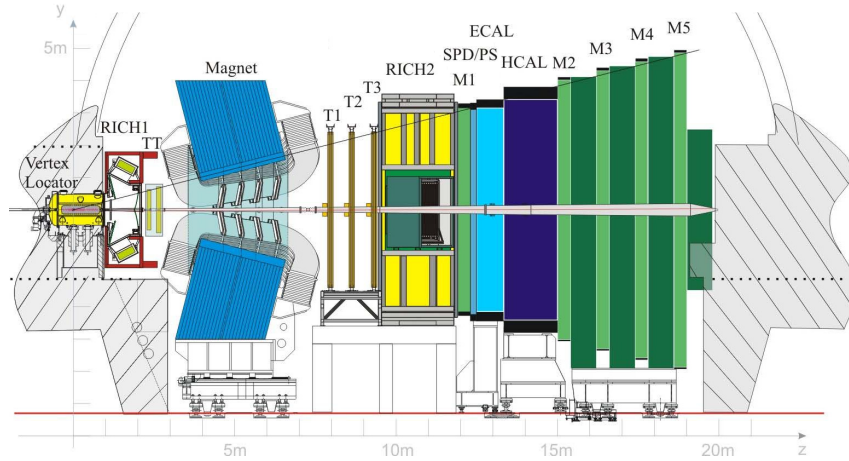


Figure 3: A cross-section of the LHCb detector. The following can be seen: the Vertex Locator (VELO), the Ring Imaging Cherenkov (RICH) detectors, the tracking stations (TT,T1-3), the magnet, the Scintillating Pad Detector (SPD), the Preshower Detector (PS), the hadronic and electromagnetic calorimeters (HCAL and ECAL) and the muon stations (M1-5).

4. Time-integrated a_{fs}^s

4.1. Analysis strategy

In this analysis decays of $B_s^0 \rightarrow D_s \mu \nu$ are selected, where $D_s \rightarrow \phi(K^+ K^-) \pi^\pm$. Using these events the un-tagged final state charge asymmetry A_{meas}^s is measured as in equation 1:

$$A_{meas}^q = \frac{N(D_q^- \mu^+) - N(D_q^+ \mu^-) \times \frac{\varepsilon(D_q^- \mu^+)}{\varepsilon(D_q^+ \mu^-)}}{N(D_q^- \mu^+) + N(D_q^+ \mu^-) \times \frac{\varepsilon(D_q^- \mu^+)}{\varepsilon(D_q^+ \mu^-)}}. \quad (1)$$

Here $N(D_q^\mp \mu^\pm)$ is the number of $D_q \mu$ combinations with the given charges. The ratio of efficiencies, $\varepsilon(D_q^- \mu^+) / \varepsilon(D_q^+ \mu^-)$, corrects for any differences in efficiency for the two channels. The measured asymmetry is related to a_{fs}^s by

$$A_{meas}^q = \frac{a_{fs}^q}{2} + \left(A_p + \frac{a_{fs}^q}{2} \right) \frac{\int_0^\infty e^{-\Gamma_q t} \cos(\Delta m_q t) \varepsilon(t) dt}{\int_0^\infty e^{-\Gamma_q t} \cosh\left(\frac{\Delta \Gamma_q t}{2}\right) \varepsilon(t) dt}, \quad (2)$$

where $\varepsilon(t)$ is the efficiency of selecting an event with decay time, t . For semi-leptonic B_s decays in LHCb, the ratio of integrals in equation 2 is approximately 0.002, as determined from simulation [5]. The B_s production asymmetry, A_p , is $\sim 1\%$ [6] and so the the second term in

equation 2 is of order 10^{-5} . Thus this term is assumed to be negligible, which leads to the approximation

$$A_{meas}^s = \frac{N(D_s^- \mu^+) - N(D_s^+ \mu^-) \times \frac{\varepsilon(D_s^- \mu^+)}{\varepsilon(D_s^+ \mu^-)}}{N(D_s^- \mu^+) + N(D_s^+ \mu^-) \times \frac{\varepsilon(D_s^- \mu^+)}{\varepsilon(D_s^+ \mu^-)}} \approx \frac{a_{fs}^s}{2}. \quad (3)$$

4.2. Signal Yield

In order to count the number of selected signal events in the sample, fits are performed to the $KK\pi$ mass spectra. The sample is split by charge of the muon and by the magnet polarity to correct for any charge asymmetry caused by the detector. The two mass peaks are described by triple Gaussians while the backgrounds are described by second-order polynomials. The selection requires the invariant mass of the KK combinations to be within 20 MeV of the ϕ mass.

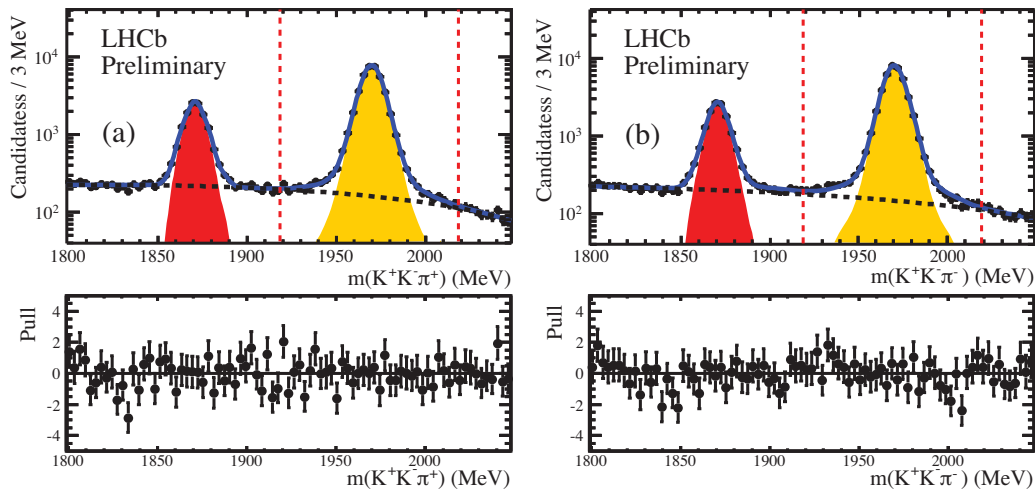


Figure 4: Invariant mass of (a) the $K^+K^-\pi^+$ combinations and (b) the $K^+K^-\pi^-$ combinations, recorded with magnet up polarity. The red dashed lines show the signal regions. The yellow shaded area is the D_s signal PDF, the red shaded region is the D^\pm mass peak PDF, the black dashed line shows the background PDF and the blue line is the sum of these three.

4.3. Detection Efficiencies

The results of the fits allow $N(D_s^\mp \mu^\pm)$ to be measured, which needs to be corrected by the efficiency ratio $\varepsilon(D_s^- \mu^+)/\varepsilon(D_s^+ \mu^-)$. To do this, the efficiency is broken down into several parts:

$$\varepsilon(D_s^\mp \mu^\pm) = \varepsilon_{id}(K^\pm K^\mp) \times \varepsilon_{tr}(K^\pm K^\mp) \times \varepsilon_{id}(\pi^\mp) \times \varepsilon_{tr}(\pi^\mp) \times \varepsilon_{id}(\mu^\pm) \times \varepsilon_{tr}(\mu^\pm) \times \varepsilon_{tg}(D_s^\mp \mu^\pm). \quad (4)$$

Due to the similarity between the K^+ and K^- momentum spectra, from the decay of the ϕ resonance, the kaon identification efficiency, $\varepsilon_{id}(K^\pm K^\mp)$, is the same for both $D_s^+ \mu^-$ and $D_s^- \mu^+$. Thus these terms cancel in the ratio. The kaon tracking efficiencies, $\varepsilon_{tr}(K^\pm K^\mp)$, also cancel. The pion identification efficiency, $\varepsilon_{id}(\pi^\mp)$, is unity since no particle identification requirements are made on the pion. The other efficiencies do not cancel between charge states leaving the pion tracking efficiency, $\varepsilon_{tr}(\pi^\mp)$, the muon identification efficiency, $\varepsilon_{id}(\mu^\pm)$, the muon tracking efficiency, $\varepsilon_{tr}(\mu^\pm)$, and the trigger efficiency, $\varepsilon_{tg}(D_s^\mp \mu^\pm)$, to be studied in more detail.

To measure the pion tracking efficiency one can select partially reconstructed decays of $D^{*\pm} \rightarrow \pi^+ D^0 (K^- \pi^+ \pi^+ \pi^-)$ [7], where one of the pions from the D^0 is missing or ignored, and then fully reconstruct the decay using only kinematics. The pion tracking efficiency is then the fraction of such events in which the additional pion is actually detected. Figure 5 shows that

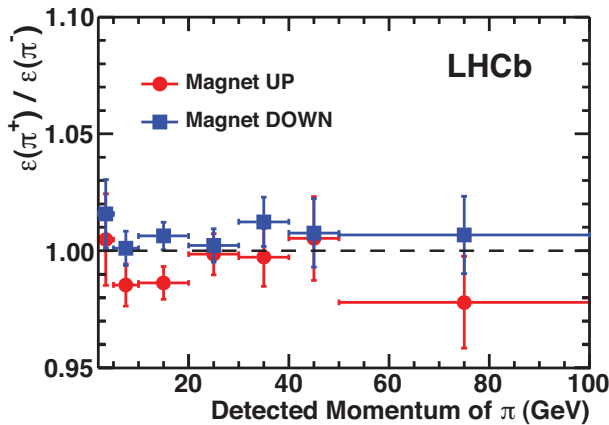


Figure 5: The ratio of π^+ and π^- tracking efficiencies as a function of pion momentum, split by magnet polarity. Data with red circles were taken with the magnet polarity in the up direction, while data with blue squares were taken with the magnet polarity in the down direction.

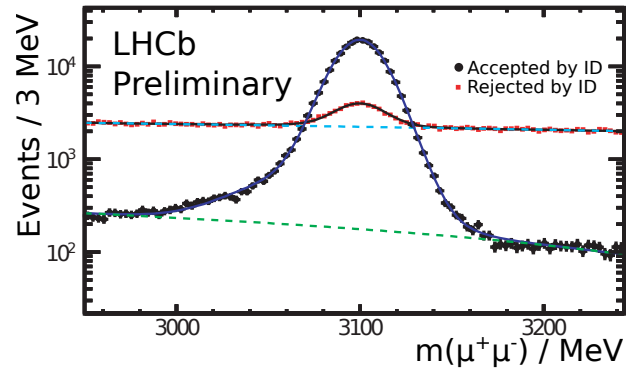


Figure 6: Invariant mass of the di-muon combination, split by those that pass or fail the muon identification cuts. The dashed green line shows the background PDF used and the solid lines are the sum of background and signal PDFs. The black points and blue line represent events which pass the muon identification cuts, while the red squares and black line represent those events which failed the same cuts.

the pion tracking efficiency ratio does not depend on the pion momentum and thus any tracking efficiency difference between the π^+ and π^- will cancel with the tracking efficiency difference between the μ^- and μ^+ . Thus $\varepsilon(D_s^\mp \mu^\pm)$ is reduced to $\varepsilon_{\text{id}}(\mu) \times \varepsilon_{\text{tg}}(D_s^\mp \mu^\pm)$, since all other terms cancel.

The remaining two efficiencies are measured using a tag-and-probe technique. Two samples of $J/\psi \rightarrow \mu^+ \mu^-$ candidates are selected using two different selection algorithms. These samples and the signal sample have different momentum spectra, so the data are divided into 50 bins of p , p_x and p_y , in which $\varepsilon_{\text{id}}(\mu)$ and $\varepsilon_{\text{tg}}(D_s^\mp \mu^\pm)$ are measured. In the J/ψ candidate selection, one of the muons is identified as a muon; this is the tag muon. The trigger is required to be independent of the second muon, known as the probe muon. This means the event would have been triggered regardless of whether the probe muon was present. The probe muon is then required to be identified as a muon. The number of J/ψ signal events which pass and fail this last requirement are counted, from which $\varepsilon_{\text{id}}(\mu)$ is measured. The J/ψ events are counted by fitting the invariant mass of the di-muon combinations as shown in figure 6. A similar process is performed for each level of the trigger. Figure 7 shows the relative efficiency of μ^+ compared to μ^- for the hardware trigger as a function of the muon momentum.

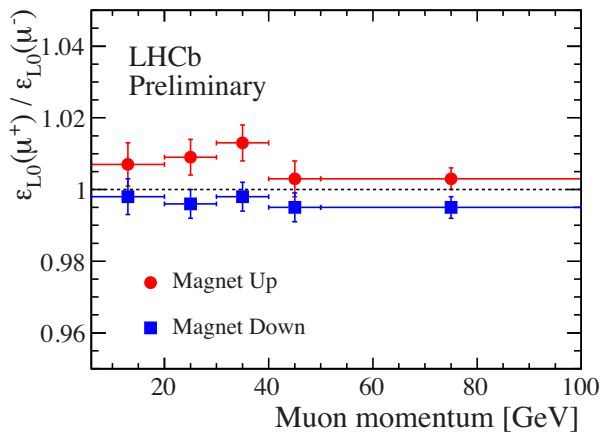


Figure 7: The ratio of μ^+ and μ^- hardware trigger efficiencies as a function of muon momentum, split by magnet polarity. Data with red circles were taken with the magnet polarity in the up direction, while data with blue squares were taken with the magnet polarity in the down direction.

Table 1: Sources of systematic uncertainties on the measured value of A_{meas}^s .

| Systematic uncertainty source | $\sigma(A_{meas}^s), \%$ |
|--|--------------------------|
| Statistical uncertainty on efficiency ratios | 0.10 |
| Signal modelling in D_s^+ mass fit | 0.06 |
| Momentum difference between π and μ | 0.06 |
| Background from other b -hadrons | 0.05 |
| Muon Corrections | 0.05 |
| Bias in muon trigger | 0.05 |
| Momentum difference between K^+ and K^- | 0.02 |
| Varying run conditions | 0.01 |
| Muon mis-ID | 0.01 |
| Total | 0.16 |

4.4. Systematic Uncertainties

Table 1 lists all effects which contribute to the total systematic uncertainty. The largest contribution of 0.10% comes from the statistical uncertainty on the efficiency correction ratios. The next largest uncertainty comes from varying the $KK\pi$ fit model. This causes variations in the number of signal events, resulting in a change of the central value by up to 0.06%. Momentum spectra of the μ^\pm and π^\mp are different, so the tracking efficiencies may not cancel exactly, resulting in a 0.06% uncertainty. Small amounts of background are selected along with the signal; most important are decays of $b \rightarrow c\bar{c}s$ where a D_s originates from a virtual W decay and the muon comes from a semi-leptonic decay of a charmed hadron, for which a 0.05% uncertainty is assigned. The uncertainty on the muon correction is estimated by comparing the differences between the two J/ψ samples, resulting in a 0.05% uncertainty. Studies of a muon software trigger has shown a bias which was corrected with a 0.09% uncertainty. In the signal sample 60% of the events pass this trigger, so an uncertainty of 0.05% is assigned.

4.5. Results

LHCb collected 447 pb^{-1} of magnet up data and 595 pb^{-1} of magnet down data in 2011. The corrected asymmetry is measured in each kinematic bin and a weighted average is taken for each magnet polarity. The arithmetic average is taken between the two magnet polarities, as this has the effect of cancelling any possible residual biases after correction. The resulting asymmetry is measured to be:

$$A_{meas}^s = (-0.12 \pm 0.27 \pm 0.17)\%,$$

giving

$$a_{fs}^s = (-0.24 \pm 0.54 \pm 0.33)\%.$$

This result is compatible with the Standard Model prediction. Figure 8 compares this result to the Standard Model prediction and previous measurements.

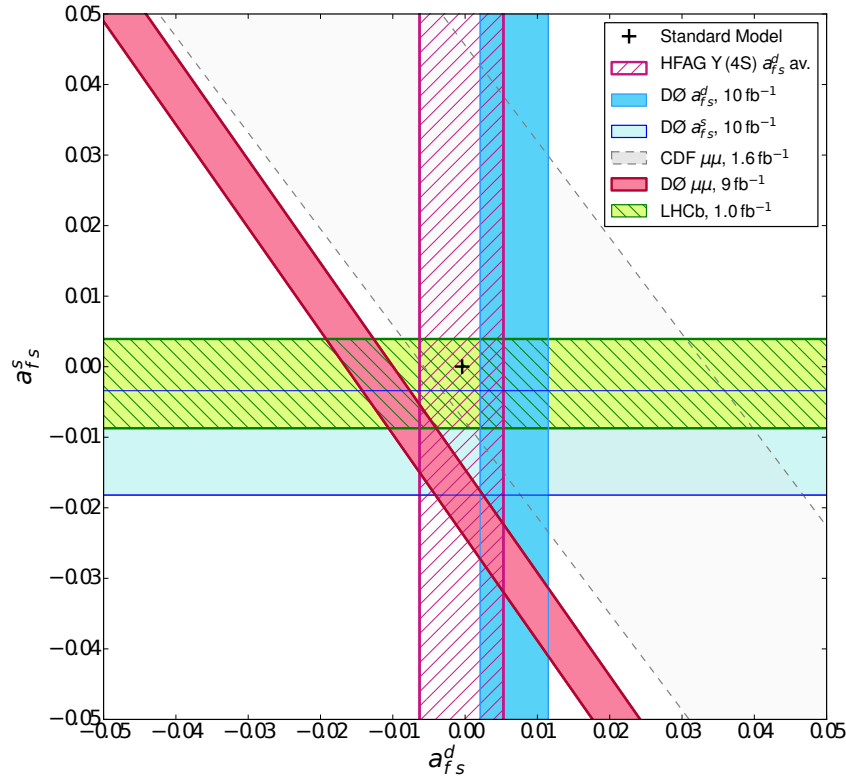


Figure 8: Plot in the $a_{fs}^s - a_{fs}^d$ plane showing CDF and DØ measurements along with an average of the B -factory measurements from HFAG and the Standard Model prediction. On top of these the LHCb time-integrated a_{fs}^s result is shown in green.

5. Time-dependent $a_{fs}^s \pm a_{fs}^d$

In a future analysis the difference and sum of a_{fs}^s and a_{fs}^d will be measured using $B_d^0 \rightarrow D\mu\nu$ and $B_s^0 \rightarrow D_s\mu\nu$ decays with $D_q \rightarrow KK\pi$. To measure the sum and difference, the data are fitted in three dimensions: decay time of the B_q , $KK\pi$ mass and muon charge. However there are neutrinos in these semi-leptonic B_q decays, which cannot be detected by LHCb, so the momentum of the B cannot be fully reconstructed. To correct for this and measure the decay time of the B_q , a statistical Monte Carlo based correction is used, called k -factor [8]. The decay time distributions of the B_q are fitted with,

$$\Gamma_{\pm}^d(t) = e^{-\Gamma_d t} \left[(2 \pm x_1^d) \cosh\left(\frac{\Delta\Gamma_d t}{2}\right) \pm x_3^d \cos(\Delta m_d t) \right] \quad \text{and} \quad \Gamma_{\pm}^s(t) = e^{-\Gamma_s t} \left[(2 \pm x_1^s) \cosh\left(\frac{\Delta\Gamma_s t}{2}\right) \right],$$

where the \pm indicates the muon charge and three asymmetries are measured: a time-averaged B_s asymmetry, x_1^s , a time-averaged B_d asymmetry, x_1^d , and an asymmetry in the B_d oscillations, x_3^d . These are related to a_{fs}^q by $x_1^s = 2A_c + a_{fs}^s$, $x_1^d = 2A_c + a_{fs}^d$ and $x_3^d = 2A_p - a_{fs}^d$, where A_c is the detection asymmetry and A_p is the production asymmetry. These measured asymmetries are combined in different ways to extract the physics quantities. The difference, $\Delta = (x_1^s - x_1^d)/2 = (a_{fs}^s - a_{fs}^d)/2$, eliminates the detector asymmetry. The sum, $\Sigma = (x_1^s + x_1^d)/2 = 2A_c + (a_{fs}^s + a_{fs}^d)/2$,

however requires a measurement of the detector asymmetry to extract the physics parameter. Finally the asymmetry in the B_d oscillations, x_3^d , is measured directly, but will have the largest uncertainty due to the the relatively large uncertainty of the production asymmetry.

These three measurements can be combined to give a strong constraint on the $a_{fs}^s - a_{fs}^d$ plane. Furthermore, by including B flavour tagging [9], a B_q mixing measurement can also be made with these events to determine Δm_q .

6. Time-dependent a_{fs}^d

Another future analysis will select $B_d^0 \rightarrow D\mu\nu$, with $D \rightarrow K\pi\pi$. This D decay is Cabibbo allowed, unlike the $D \rightarrow KK\pi$ decay in the time-dependent $a_{fs}^s \pm a_{fs}^d$ analysis, and so more B_d events are available to this analysis. A similar method is used to the time-integrated a_{fs}^s measurement, where the final state charge asymmetry is measured, which is shown in equations 1 and 2. However due to the slow oscillations of the B_d , the integral ratio in the second term of equation 2 is no longer small. This means the B decay time distribution must be fitted, as with the $a_{fs}^s \pm a_{fs}^d$ analysis. The ratio $\varepsilon(D^-\mu^+)/\varepsilon(D^+\mu^-)$ needs to be measured as before, but this time $\varepsilon(K^\pm\pi^\mp)$ also needs to be measured since the D no longer decays via $\phi \rightarrow KK$. To do this the relative efficiency of $K^\pm\pi^\mp$ is measured using the decays shown in equation 5:

$$\frac{\varepsilon(K^+\pi^-)}{\varepsilon(K^-\pi^+)} = \frac{N(D^- \rightarrow K^+\pi^-\pi^-)}{N(D^+ \rightarrow K^-\pi^+\pi^+)} \times \frac{N(D^+ \rightarrow K_s^0\pi^+)}{N(D^- \rightarrow K_s^0\pi^-)}. \quad (5)$$

This efficiency correction is applied along with the pion and muon corrections, which are determined as in the time-integrated analysis. These three efficiencies are combined to give $\varepsilon(D^-\mu^+)/\varepsilon(D^+\mu^-)$, which is input to the B_d decay time fitter to determine a_{fs}^d .

7. Conclusion

The \mathcal{CP} violating parameter $a_{fs}^s = (-0.24 \pm 0.54 \pm 0.33)\%$ has been determined using a time-integrated method. This measurement is compatible with previous measurements as well as the Standard Model prediction. LHCb is pursuing two further measurements on the $a_{fs}^s - a_{fs}^d$ plane, which will cross-check the current and previous measurements.

References

- [1] A. Lenz 2011 A simple relation for B_s -mixing *Phys. Rev. D* **84** 031501
- [2] V. M. Abazov *et al.* DØ Collaboration 2011 Measurement of the anomalous like-sign dimuon charge asymmetry with 9 fb^{-1} of $p\bar{p}$ collisions *Phys. Rev. D* **84** 052007
- [3] R. Antunes-Nobrega, *et al.* LHCb collaboration 2003 *LHCb Reoptimised Detector Design and Performance, Technical Design Report 9* CERN LHCC 2003-030
- [4] P. M. Bjørnstad 2011 Performance of the LHCb Vertex Locator *JINST* **6** C12024
- [5] R. Aaij *et al.* LHCb collaboration 2012 Measurement of the flavour-specific CP violating asymmetry a_{sl}^s in B_s decays *PoS(ICHEP2012)*
- [6] R. Aaij *et al.* LHCb collaboration 2012 First evidence of direct CP violation in charmless two-body decays of B_s^0 mesons *Phys. Rev. Lett.* **108** 201601
- [7] R. Aaij *et al.* LHCb collaboration 2012 Measurement of the $D_s^+ - D_s^-$ production asymmetry in 7 TeV pp collisions *Phys. Lett. B* **713** 186-95
- [8] A. Abulencia *et al.* CDF collaboration 2006 Measurement of the $B_s^0 - \bar{B}_s^0$ oscillation frequency *Phys. Rev. Lett.* **97** 062003
- [9] R. Aaij *et al.* LHCb collaboration 2012 Opposite-side flavour tagging of B mesons at the LHCb experiment *Eur. Phys. J. C* **72** 2022